PHYSICAL REVIEW D **87,** 115024 (2013)

# Search for $Z'$ via $ZH$ associated production at the LHC

Hong-Lei Li,[1,2,*] Zong-Guo Si,[3] Xiu-Yi Yang,[3,4] Zhong-Juan Yang,[5] and Ya-Juan Zheng[6]

[1]*School of Physics and Technology, University of Jinan, Jinan Shandong 250022, China*
[2]*Department of Physics, University of the Chinese Academy of Sciences, Beijing 100049, China*
[3]*School of Physics, Shandong University, Jinan Shandong 250100, China*
[4]*School of Science, University of Science and Technology Liaoning, Anshan, Liaoning 114051, China*
[5]*School of Physics and Chemistry, Henan Polytechnic University, Jiaozuo Henan, 454003, China*
[6]*CASTS, CTS and Department of Physics, National Taiwan University, Taipei 10617, China*

(Received 9 May 2013; published 21 June 2013)

Many new physics models predict the existence of an extra neutral gauge boson ($Z'$). Inspired by the recent development in the Higgs search, we study the properties of $Z'$ via the Higgs and $Z$-boson associated production. The couplings of $Z'$ to quarks can be investigated through the $pp \to Z' \to ZH \to l^+l^- b\bar{b}$ process, which also provides an extraordinary signal for understanding the properties of the $Z'ZH$ interaction. The standard model background processes can be significantly suppressed by adopting appropriate kinematic cuts. The charged lepton angular distributions are related to the ratio of the chiral couplings of $Z'$ to quarks via the $Z'ZH$ interaction.

DOI: 10.1103/PhysRevD.87.115024 PACS numbers: 14.70.Pw, 12.60.Cn, 14.70.Hp, 14.80.Bn

## I. INTRODUCTION

The ATLAS and CMS collaborations at the LHC have recently reported the discovery of a standard model (SM)-like Higgs boson with mass around 125 GeV [1,2]. It is timely to study the physics related to the Higgs boson within and beyond the SM. In some of the simplest extensions of the SM, such as the simple extra $U(1)'$ gauge symmetry [3–5], the left-right models [6–10], and even string theory [11,12], etc., a new neutral gauge boson $Z'$ is introduced. The crucial test for these models is to search for the $Z'$ production signal and to study its related properties.

The $Z'$ boson is widely investigated at both LEP and hadron colliders. Constraints on the $Z'$ mass and coupling strength with the SM particles have been obtained through the $e^+e^- \to f\bar{f}$ process at the electron-positron collider [13–15]. In particular, the precision measurements at the $Z$ pole give a limit on the $Z - Z'$ mixing [16]. Bounds on several models containing extra neutral gauge boson have been set by both the CDF and D0 experiments by measuring high-energy lepton-pair production cross sections at the Tevatron [17,18]. Due to the high luminosity and collision energy, the LHC implies a more promising potential to observe heavy gauge bosons. More recently, the $e^+e^-$, $\mu^+\mu^-$, $\tau^+\tau^-$ final states, along with the $Z'$ decay into jets which suffers from large QCD backgrounds, have also been studied at the LHC [19]. A $Z'$ boson in association with vector bosons as well as top-quark production is explored at the LHC, and is important for disentangling the origin of electroweak symmetry breaking.

For theoretical reviews of $Z'$ boson physics, we refer to Refs. [20–22]. Based on specific new physics models, $Z'$ phenomenological signatures have been studied in the literature [23–30]. In the extensively studied Drell-Yan process, clear signatures for the $Z'$ boson can be reconstructed, while it is no picnic investigating the properties of $Z'$ coupling to quarks because of the inevitable mixing from its coupling to leptons. Another important process is $pp \to Z' \to ZH$, which can offer an opportunity to study the properties of $Z'q\bar{q}$ as well as the $Z'ZH$ interaction.

In this paper, we investigate the $Z'$ signal via the $ZH$ associated production at the LHC with the subsequent decay of $Z \to l^+l^-$ and $H \to b\bar{b}$, which will shed light on the understanding of $Z'q\bar{q}$ and $Z'ZH$ interactions. It shows that the couplings of the $Z'$ boson to quarks are related to the charged lepton angular distributions through the $Z'ZH$ interaction.

This paper is organized as follows. In Sec. II, experimental constraints and the theoretical framework are briefly introduced. Section III is devoted to the numerical analysis of $Z'$-mediated $ZH$ production at the LHC and the corresponding SM backgrounds are considered as well. Finally, a short summary is given.

## II. EXPERIMENTAL CONSTRAINTS AND THEORETICAL FRAMEWORK

In this section we collect the constraints on the $Z'$ mass from $pp$ and $p\bar{p}$ colliders. The CMS collaboration excludes leptophobic $Z'$ resonances of masses $m_{Z'} <$ 1.3 TeV for a width $\Gamma_{Z'} = 0.012 m_{Z'}$ in a search for heavy resonances decaying into $t\bar{t}$ pairs with subsequent leptonic decay of both top-quark and antiquark processes [31]. The ATLAS collaboration investigated a massive resonance decaying into $t\bar{t}$ pairs in the fully hadronic final state, and excludes the leptophobic $Z'$ boson model with masses $0.70 < m_{Z'} < 1.00$ TeV and $1.28 < m_{Z'} < 1.32$ TeV as well [32]. Based on the analysis of $pp$ collisions at a

*sps_lihl@ujn.edu.cn

 

center-of-mass energy of 8 TeV corresponding to an integrated luminosity of approximately $5.9(e^+e^-)/6.1(\mu^+\mu^-)$ fb$^{-1}$, a sequential SM $Z'$ boson is excluded at 95% C.L. for masses below 2.39 TeV in the electron channel ($e^+e^-$), 2.19 TeV in the muon channel ($\mu^+\mu^-$), and 2.49 TeV in the two channels combined ($l^+l^-$) [33]. Both D0 and CDF collaborations search for a heavy neutral gauge boson in the $e^+e^-$ channel of $p\bar{p}$ collisions at $\sqrt{s} = 1.96$ TeV. A lower mass limit of 1.023 TeV and 0.963 TeV for the sequential SM $Z'$ boson is presented, respectively, [17,18]. Using constraints from the precision electroweak (EW) data, the lower mass limit on an extra neutral boson $Z'_{LR}$ in left-right symmetric models is around 1 TeV [34]. The results for various $E_6$-motivated $Z'$ bosons are reported from ATLAS with a lower mass limit of 1.49–1.64 TeV [35], and a mass less than 2.09–2.24 TeV is excluded by CMS. According to the CMS analysis, a $Z'$ with SM-like couplings can be excluded below 2.59 TeV and the superstring-inspired $Z'_\psi$ below 2.26 TeV [36]. However, the $Z'$ mass constraints discussed above depend on the free parameters, such as its decay width and branching ratios, and still can be loosened to some extent.

Considering the existence of $Z'$, the weak neutral current interactions related to the fermions are described by the Lagrangian

$$-\mathcal{L}_{\rm NC} = [\bar{q}\gamma^\mu(g_L^q P_L + g_R^q P_R)q + \bar{l}\gamma^\mu(g_L^l P_L + g_R^l P_R)l]Z_\mu + [\bar{q}\gamma^\mu(g_L^{\prime q} P_L + g_R^{\prime q} P_R)q + \bar{l}\gamma^\mu(g_L^{\prime l} P_L + g_R^{\prime l} P_R)l]Z'_\mu, \quad (1)$$

where $P_{L,R} = (1 \mp \gamma_5)/2$ are the left and right chiral projections and $g^i_{L,R}$ ($g'^i_{L,R}$) are the chiral couplings of the $Z$ ($Z'$) boson to corresponding fermions. $g^i_{L,R} = g/\cos\theta_W(T^i_{3L,R} - \sin^2\theta_W Q^i)$ and $T_3$ ($Q$) is the third component of weak isospin (charge) of the corresponding particle. We neglect the $Z - Z'$ mixing in the following, and refer to, e.g., Refs. [37–41] and references therein for corresponding discussions. From Eq. (1), one can obtain the $Z'$ decay width into a fermion,

$$\Gamma_{Z'\to f\bar{f}} = \frac{C_f m_{Z'}}{24\pi}(g_L^{\prime f2} + g_R^{\prime f2}), \quad (2)$$

$$\Gamma_{Z'\to t\bar{t}} = \frac{m_{Z'}}{8\pi}\left(1 - \frac{m_t^2}{m_{Z'}^2}\right)\sqrt{1 - \frac{4m_t^2}{m_{Z'}^2}}(g_L^{\prime t2} + g_R^{\prime t2}), \quad (3)$$

where $C_f$ is the color factor (1 for leptons and 3 for quarks), $m_t$ is the mass of the top quark, and the light fermion masses have been neglected.

The $Z'ZH$ interaction can be extracted from

$$-\mathcal{L}_{\rm kin} \equiv g_{ZZH}Z_\mu Z^\mu H + g_{Z'ZH}Z'_\mu Z^\mu H + g_{Z'Z'H}Z'_\mu Z'^\mu H + \cdots, \quad (4)$$

where $g_{VVH}$ stands for the coupling strength of the $VVH$ interaction. We set $g_{Z'ZH} = g_{ZZH}/2$ and $g_{ZZH} = gm_Z/\cos\theta_W$ in the following discussion. Thus for a $Z'$ boson with $m_{Z'} > m_H + m_Z$, the partial decay width is

$$\Gamma_{Z'\to ZH} = \frac{g^2_{Z'ZH}}{48\pi m^3_{Z'}}\left[2 + \frac{(m^2_{Z'} + m_Z^2 - m_H^2)^2}{4m^2_{Z'}m_Z^2}\right] \times \sqrt{[m^2_{Z'} - (m_Z + m_H)^2][m^2_{Z'} - (m_Z - m_H)^2]}. \quad (5)$$

We show the $Z'$-boson decay branching ratio with various mass values in Fig. 1. In this paper, the couplings of $Z'$ to fermions are set to be the same as those of the $Z$ boson without special declaration. The dominant decay channel is $Z' \to f\bar{f}$ modes. The branching ratio of the $l^+l^-$ channel is about thirty percent—which can be a good channel for the discovery of the $Z'$ boson at the LHC due to the outstanding detector performance—and the $ZH$ channel branching ratio is about one percent.

However, at the LHC Higgs associated with $Z$-boson production plays an important role and the $q\bar{q} \to Z' \to ZH$ process contributes to it. We display the cross section of $ZH$ associated production at the LHC in Fig. 2. The cross section of $ZH$ production from the $Z'$ boson is above 100 (1) fb for $m_{Z'} = 1$ (1.5) TeV at the LHC with $\sqrt{s} = 14$ TeV, which leads to considerable effects compare with that from the $Z$ boson, so it is possible to study $ZH$ associated processes via $Z'$ production at the LHC.

With the $Z$-boson leptonic decay modes, the corresponding matrix element square for the process

$$q(p_1)\bar{q}(p_2) \to Z/Z' \to ZH \to l^+(p_3)l^-(p_4)H \quad (6)$$

is given by

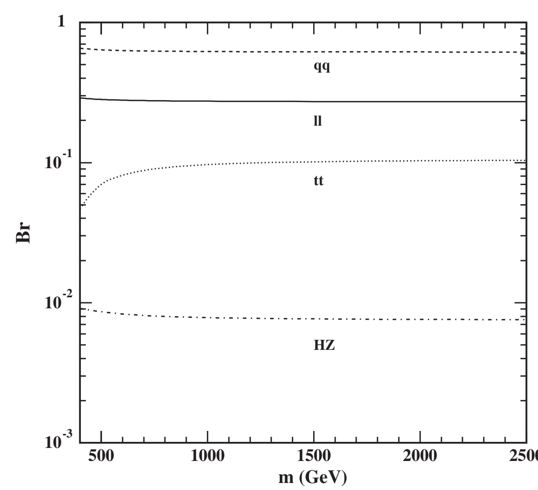


FIG. 1. $Z'$ decay branching ratio versus $m_{Z'}$.

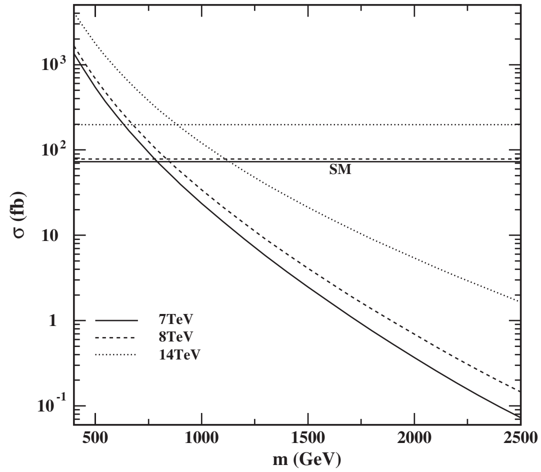


FIG. 2. The cross section for the process $pp \to Z' \to ZH$ with $m_{Z'}$ at (a) 7 TeV, (b) 8 TeV, and (c) 14 TeV at the LHC. The straight lines stand for the contribution from $pp \to Z \to ZH$.

$$|\mathcal{M}|^2 = \frac{16}{N_c N_s \mathcal{P}_{2Z}} \Big\{ \frac{g^2_{Z'ZH}}{\mathcal{P}_{1Z'}} [(g_L^{l2} g_L^{\prime q2} + g_R^{l2} g_R^{\prime q2})\mathcal{A} + (g_R^{l2} g_L^{\prime q2} + g_L^{l2} g_R^{\prime q2})\mathcal{B}] + \frac{g^2_{ZZH}}{\mathcal{P}_{1Z}} [(g_L^{l2} g_L^{q2} + g_R^{l2} g_R^{q2})\mathcal{A} + (g_R^{l2} g_L^{q2} + g_L^{l2} g_R^{q2})\mathcal{B}] + \frac{g_{ZZH} g_{Z'ZH} \mathcal{T}}{\mathcal{P}_{1Z} \mathcal{P}_{1Z'}} \times [(g_L^{l2} g_L^{q} g_L^{\prime q} + g_R^{l2} g_R^{q} g_R^{\prime q})\mathcal{A} + (g_R^{l2} g_L^{q} g_L^{\prime q} + g_L^{l2} g_R^{q} g_R^{\prime q})\mathcal{B}] \Big\}, \tag{7}$$

with $\mathcal{T} = 2(s_1 - m_Z^2)(s_1 - m_{Z'}^2) + \Gamma_Z m_Z \Gamma_{Z'} m_{Z'}$, $\mathcal{A} = (p_1 \cdot p_3)(p_2 \cdot p_4)$, $\mathcal{B} = (p_1 \cdot p_4)(p_2 \cdot p_3)$, $\mathcal{P}_{ij} = (s_i - m_j^2)^2 + \Gamma_j^2 m_j^2$, $i = 1, 2$, and $j = Z, Z'$, where $s_1 = (p_1 + p_2)^2$ is the energy square in the center-of-mass system, $s_2 = (p_3 + p_4)^2$ is the invariant mass square of the final leptons, and $N_c = 3$ and $N_s = 4$ are the color and spin factors, respectively. From the expression of Eq. (7), one can notice that the couplings of $Z'$ to quarks are related to the angle between the momentum of the lepton and the initial quark.

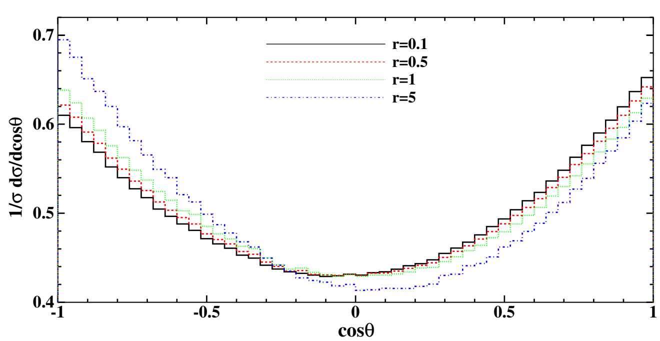


FIG. 3 (color online). The angular distribution for the charged lepton ($l^-$). The mass of $Z'$ is set at 1.5 TeV.

Considering the Higgs hadronic decay, one can find that the partonic-level final state is $l^+ l^- b\bar{b}$. Following the analytical method in our previous works on new boson production [23,24,42–46], we focus on the property of the final lepton angular distribution. The total momentum of the final-particle system is defined as $\mathbf{p} = \mathbf{p_b} + \mathbf{p_{\bar{b}}} + \mathbf{p_{l^+}} + \mathbf{p_{l^-}}$ in the laboratory frame. The angle between the three-momentum $\mathbf{p}^*_{l^-}$ of the lepton in the $Z$-boson rest frame and $\mathbf{p}$ is

$$\cos\theta = \frac{\mathbf{p}^*_{l^-} \cdot \mathbf{p}}{|\mathbf{p}^*_{l^-}| \cdot |\mathbf{p}|}. \tag{8}$$

We show distributions of $1/\sigma d\sigma/d\cos\theta$ versus $\cos\theta$ with different $r$ values in Fig. 3, where $r$ is defined as $r = g_L^{\prime q}/g_R^{\prime q}$. To give a simplified picture, we set $g_L^{\prime u} = g_L^u$ and $g_L^{\prime u}/g_L^{\prime d} = g_L^u/g_L^d$. One can find that the charged leptons have a large probability to move against the $Z'$-boson boosting direction with large $r$. Therefore, from this kind of angular distribution, one can extract useful information for understanding the $Z' q\bar{q}$ interaction.

## III. COLLIDER ANALYSIS

$Z'$-boson searches at the LHC have been performed by the ATLAS and CMS collaborations in the dilepton final states. $ZH$ production via the $Z$ boson was also elaborately investigated for the search for the Higgs boson, and thus the $Z'$-mediated production

$$pp \to Z' \to ZH \to l^+ l^- b\bar{b} \tag{9}$$

will be an important process for Higgs searches beyond the SM. The transverse-momentum distributions of the jets and leptons are shown in Figs. 4(a) and 4(b). In order to identify the isolated jet (lepton), we define the angular separation between particle $i$ and particle $j$ as

$$\Delta R_{ij} = \sqrt{\Delta\phi_{ij}^2 + \Delta\eta_{ij}^2}, \tag{10}$$

where $\Delta\phi_{ij} = \phi_i - \phi_j$ and $\Delta\eta_{ij} = \eta_i - \eta_j$. $\phi_i$ ($\eta_i$) denotes the azimuthal angle (rapidity) of the related jet or lepton.

To be more realistic, the simulation at the detector is performed by smearing the leptons and jets energies' according to the assumption of the Gaussian resolution parametrization,

$$\frac{\delta(E)}{E} = \frac{a}{\sqrt{E}} \oplus b, \tag{11}$$

where $\delta(E)/E$ is the energy resolution, $a$ is a sampling term, $b$ is a constant term, and $\oplus$ denotes a sum in quadrature. We take $a = 5\%$, $b = 0.55\%$ for leptons and $a = 100\%$, $b = 5\%$ for jets, respectively, [47,48].

The corresponding distributions for $\Delta R = \min(\Delta R_{ij})$ are shown in Fig. 4(c). Due to the large mass splitting between the $Z'$ and the Higgs as well as the $Z$ boson, the

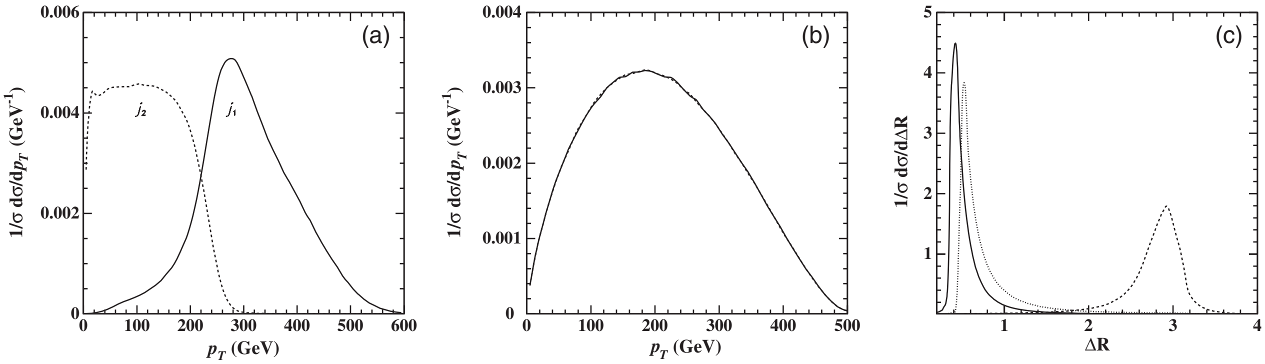


FIG. 4. (a) The transverse momentum distributions of the jets $(j_1, j_2)$ with $p_{Tj_1} > p_{Tj_2}$ at $\sqrt{s} = 14$ TeV. (b) The transverse momentum distributions of the leptons. (c) The minimal angular separation distributions between leptons (solid line), jets (dashed line), and between jets and leptons (dotted line).

mediated particles will be highly boosted and the jets (leptons) are mostly moving in the same direction as the Higgs ($Z$); meanwhile, jets are mostly moving in the opposite direction as leptons. According to the above distributions, we adopt the basic cuts (cut I)

$$p_{T_l} > 30 \text{ GeV}, \qquad p_{T_{j1}} > 100 \text{ GeV}, \qquad p_{T_{j2}} > 50 \text{ GeV},$$
$$|\eta_l| < 2.5, \qquad |\eta_j| < 3.0, \qquad \Delta R_{jl} > 2.0. \tag{12}$$

Analyzing the $l^- l^+ jj$ final state, we find that two leptons are from the $Z$ boson and two jets are from the Higgs boson. Hence, the mediate resonances can be reconstructed through the invariant masses of the jets and leptons, respectively. The invariant mass distributions reconstructed by (a) leptons, (b) jets, and (c) leptons and jets are shown in Fig. 5. We employ the invariant mass through various combinations of the final particles to constrain the mediate resonances (cut II),

$$\frac{|M_{jj} - m_H|}{m_H} \leq 10\%, \qquad \frac{|M_{ll} - m_Z|}{m_Z} \leq 10\%, \quad \text{and}$$
$$\frac{|M_{jjll} - m_{Z'}|}{m_{Z'}} \leq 10\%, \tag{13}$$

together with one of the final jets tagged as $b$-jet.

Corresponding to the final state of $l^- l^+ jj$, SM processes mediated by $ZH$, $t\bar{t}$, $ZW$, $ZZ$, $Zjj$, and $WWjj$ are the main backgrounds. To suppress the influence from the background processes, the discrepancies between signal and background processes are analyzed. Obviously, most of the cross section of $ZH$ is due to the $Z$-boson resonance, which can be cut down by adopting the final-system invariant mass cut. The decay mode $t\bar{t} \to W^+ b W^- \bar{b} \to l^+ \bar{\nu} b l^- \nu b$ is required to obtain the $l^- l^+ jj$ final state for the $t\bar{t}$ process. It shows that the charged leptons are coming from different intermediate $W$ bosons in the $t\bar{t}$ process, and thus we can set the invariant mass reconstructed by two charged leptons to be around the $Z$-boson mass to cut down the $t\bar{t}$ process as well as the $WWjj$ process. For the processes with jets, such as $Zjj$ and $WWjj$, jets are coming predominantly from QCD processes; then, the invariant mass reconstructed by the final jets leads to different distributions compared with signal processes. Besides, since we require the final jets' reconstructed invariant mass to be around the Higgs mass the $ZW$ and $ZZ$ processes can be suppressed for the mass gaps between the Higgs and $Z$ boson.

Furthermore, due to the $Z'$ mass hierarchy from the Higgs and $Z$ boson, a $Z$ boson reconstructed from the charged leptons will have a high Lorentz boost factor ($\gamma$). Thus we adopt

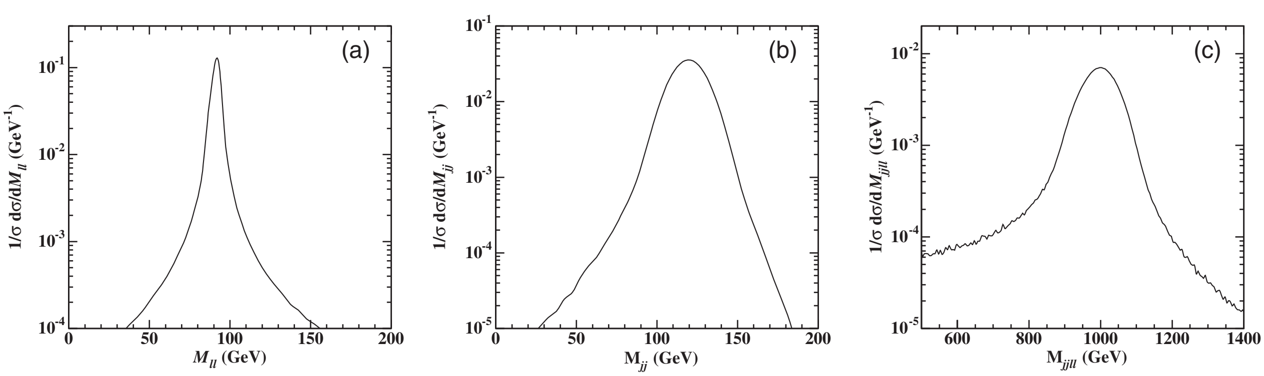


FIG. 5. The distribution for the invariant mass reconstructed from (a) leptons, (b) jets, and (c) all final-state particles.

TABLE I. The total cross section (fb) for signal and background processes before and after cuts at the $\sqrt{s} = 14$ TeV LHC with $m_{Z'} = 1$ TeV and the corresponding significance with a luminosity of 300 fb$^{-1}$.

| Process | No cut | Cut I | Cut I + II | Cut I + II + III |
|---|---|---|---|---|
| Signal | 13.3 | 4.48 | 2.78 | 2.08 |
| $ZH$(SM) | 669 | 0.30 | 0.04 | 0.03 |
| $t\bar{t}$ | $5.38 \times 10^5$ | 20.5 | 0.39 | ⋯ |
| $ZW$ | $2.76 \times 10^4$ | 2.68 | ⋯ | ⋯ |
| $ZZ$ | $1.05 \times 10^4$ | 3.13 | ⋯ | ⋯ |
| $Zjj$ | $7.37 \times 10^6$ | 855 | ⋯ | ⋯ |
| $WWjj$ | $6.88 \times 10^4$ | 10.7 | ⋯ | ⋯ |
| $S/B$ | $1.7 \times 10^{-6}$ | 0.005 | 6.46 | 69.3 |
| $S/\sqrt{B}$ | 0.08 | 2.59 | 73.4 | 208 |

$$\gamma = \frac{1}{\sqrt{1-v^2}} \geq 3.0, \tag{14}$$

referred as cut III to further suppress the backgrounds, where $v$ is the velocity of the $Z$ boson in the laboratory frame.

The total cross sections for the signal and background processes before and after cuts are listed in Table I. The dominant backgrounds from the $t\bar{t}$ and $Zjj$ cross sections are over $\mathcal{O}(10^4)$ than the signal process before cuts. After the basic kinematic cuts and the invariant-mass cuts (cut I + II), most backgrounds are significantly suppressed. The $t\bar{t}$ process will be further suppressed by cut III. With the SM $ZH$ process substantially reduced, all the backgrounds are eliminated through the three cuts, and thus the signal process can be clearly studied. The significance can reach $S/B = 69.3$ and $S/\sqrt{B} = 208$ with a luminosity of 300 fb$^{-1}$.

The cross sections for the other choice of the $Z'$ mass are also listed in Table II. It shows that more than one hundred events can be detected at the LHC with a luminosity of 300 fb$^{-1}$ for $m_{Z'} = 1.5$ TeV. The background processes can be strongly suppressed with a larger final-system invariant mass and a loose $M_{jjll}$ cut can be used to emphasize the signal. The dependence of the cross section on the coupling strength ratio of $g_{Z'ZH}$ to $g_{ZZH}$ is shown in Fig. 6. It implies that this process can be investigated in the region of $g_{Z'ZH}/g_{ZZH} > 0.02$, 0.04, 0.08, corresponding to $m_{Z'} = 1$, 1.5, 2 TeV at LHC with a luminosity of 300 fb$^{-1}$.

TABLE II. The total cross section (fb) for signal processes before and after cuts at the $\sqrt{s} = 14$ TeV LHC with $m_{Z'} = 1$, 1.5, 2 TeV.

| $m_{Z'}$ | No cut | Cut I | Cut I + II | Cut I + II + III |
|---|---|---|---|---|
| 1 TeV | 13.3 | 4.48 | 2.78 | 2.08 |
| 1.5 TeV | 9.67 | 1.14 | 0.56 | 0.42 |
| 2 TeV | 9.31 | 0.60 | 0.15 | 0.11 |

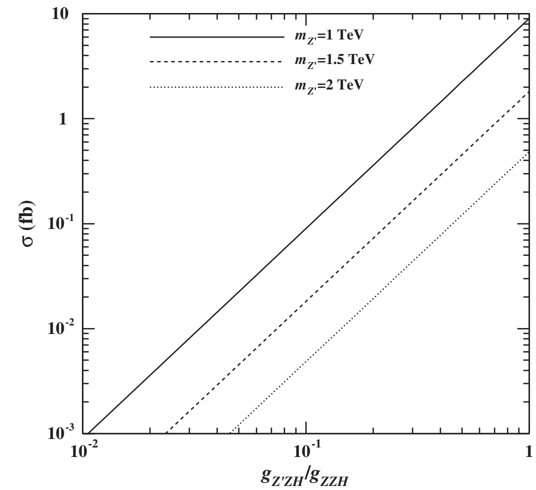


FIG. 6. The cross section for process (9) with $g_{Z'ZH}/g_{ZZH}$ at the LHC for $m_{Z'} = 1$, 1.5, 2 TeV and $r = 1$.

After adopting all the kinematic cuts, we display the $1/\sigma d\sigma/d\cos\theta$ distributions versus $\cos\theta$ for different $r$ in Fig. 7. The distributions with $|\cos\theta|$ close to zero and one are distorted by the kinematic cuts to some extent, but one can find that the charged leptons tend to move along in the opposite direction of the final system with large $r$. It is possible to utilize the angular distribution to distinguish various models including the $Z'q\bar{q}$ interaction with different chiral couplings.

Corresponding to the charged lepton angular distribution of process (9), we define a kind of forward-backward asymmetry ($A_{\rm FB}$),

$$A_{\rm FB} = \frac{\sigma(\cos\theta \geq 0) - \sigma(\cos\theta < 0)}{\sigma(\cos\theta \geq 0) + \sigma(\cos\theta < 0)}. \tag{15}$$

The cross sections and $A_{\rm FB}$ are listed in Table III. It is obvious that the forward-backward asymmetry is sensitive to different values of $r$. By increasing the value of $r$, $A_{\rm FB}$ changes from negative to positive. The absolute value of the forward-backward asymmetry becomes smaller for heavier $Z'$ with fixed $r$. The numbers in Table III show that with an integrated luminosity of 300 fb$^{-1}$ for a

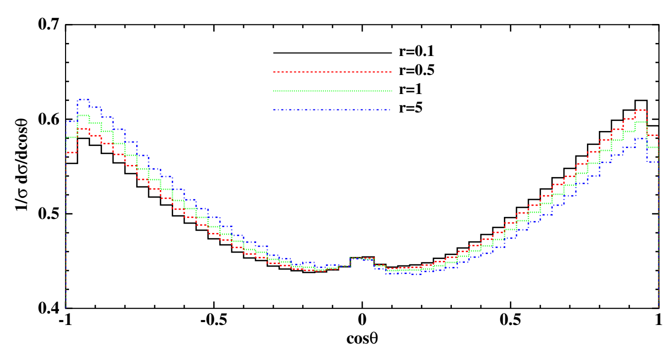


FIG. 7 (color online). The angular distribution for a charged lepton after all cuts at the LHC with $m_{Z'} = 1.5$ TeV.

TABLE III. The total cross section ($\sigma$) and forward-backward asymmetry ($A_{FB}$) after cuts at the LHC with $\sqrt{s} = 14$ TeV.

| $m_{Z'}$ (TeV) | 1 | | | | 1.5 | | | | 2 | | | |
|---|---|---|---|---|---|---|---|---|---|---|---|---|
| $r$ | $r = 0.1$ | $r = 0.5$ | $r = 1$ | $r = 5$ | $r = 0.1$ | $r = 0.5$ | $r = 1$ | $r = 5$ | $r = 0.1$ | $r = 0.5$ | $r = 1$ | $r = 5$ |
| $\sigma$ (fb) | 2.10 | 2.20 | 2.25 | 0.54 | 0.42 | 0.44 | 0.45 | 0.11 | 0.11 | 0.11 | 0.12 | 0.03 |
| $A_{FB}$ | 0.032 | 0.016 | $-0.006$ | $-0.032$ | 0.022 | 0.011 | $-0.004$ | $-0.021$ | 0.016 | 0.008 | $-0.003$ | $-0.016$ |

center-of-mass at 14 TeV, 670 (130) events can be expected for a $Z'$ mass at 1 (1.5) TeV with $r = 1$, and $A_{FB}$ can reach 0.032 ( $-$ 0.032) for $r = 0.1$ ($r = 5$) with $m_{Z'} = 1$ TeV. One can find that after the acceptance cuts, the angular distribution with respect to $\cos\theta$ and $A_{FB}$ is helpful to investigate the $Z'ZH$ interaction via $ZH$ associated production at the LHC.

## IV. SUMMARY

Many extensions beyond the SM predict the existence of a new heavy neutral gauge boson. The recently discovered SM-like Higgs boson at the LHC motivates us to investigate the $Z'ZH$ interaction. We studied the process of $pp \to Z' \to ZH$ with $Z \to l^+l^-$ and $H \to b\bar{b}$ decay modes. A massive $Z'$ boson can be reconstructed through the resonance peak that appears in the invariant mass spectrum of the final states $l^+l^-b\bar{b}$. The couplings of $Z'$ to SM fermions can be extracted from right-handed and left-handed currents, and thus the chiral coupling ratio $r$ can serve as an important parameter to specify various models. We found that the angular distribution for the final lepton can be related to $r$ via the $Z'ZH$ interaction. The backgrounds from the SM with the same final state were estimated and efficiently suppressed by the kinematic cuts. Corresponding to the angular distribution of the final-state charged lepton, we defined a forward-backward asymmetry $A_{FB}$ which is sensitive to $r$. A variety of new physics models predict a different chiral coupling ratio $r$, and thus the charged lepton angular distribution and the forward-backward asymmetry can help one to understand the $Z'ZH$ interaction and distinguish between different models.

## ACKNOWLEDGMENTS

This work is supported in part by the NSFC and NSC. The authors would like to thank Profs. X. He, S. Li, S. Bao, and Y. Jin for their useful comments and helpful discussions on this work.


[1] G. Aad *et al.* (ATLAS Collaboration), Phys. Lett. B **716**, 1 (2012).

[2] S. Chatrchyan *et al.* (CMS Collaboration), Phys. Lett. B **716**, 30 (2012).

[3] R. W. Robinett and J. L. Rosner, Phys. Rev. D **25**, 3036 (1982); **27**, 679(E) (1983).

[4] J. L. Hewett and T. G. Rizzo, Phys. Rep. **183**, 193 (1989).

[5] D. London and J. L. Rosner, Phys. Rev. D **34**, 1530 (1986).

[6] J. C. Pati and A. Salam, Phys. Rev. D **10**, 275 (1974); **11**, 703(E) (1975).

[7] R. N. Mohapatra and J. C. Pati, Phys. Rev. D **11**, 566 (1975).

[8] R. N. Mohapatra and J. C. Pati, Phys. Rev. D **11**, 2558 (1975).

[9] G. Senjanovic and R. N. Mohapatra, Phys. Rev. D **12**, 1502 (1975).

[10] R. N. Mohapatra, F. E. Paige, and D. P. Sidhu, Phys. Rev. D **17**, 2462 (1978).

[11] M. Cvetic and P. Langacker, Phys. Rev. D **54**, 3570 (1996).

[12] M. Cvetic and P. Langacker, Mod. Phys. Lett. A **11**, 1247 (1996).

[13] P. Chiappetta, J. Layssac, F. M. Renard, and C. Verzegnassi, Phys. Rev. D **54**, 789 (1996).

[14] V. D. Barger, K.-m. Cheung, and P. Langacker, Phys. Lett. B **381**, 226 (1996).

[15] K. R. Lynch, E. H. Simmons, M. Narain, and S. Mrenna, Phys. Rev. D **63**, 035006 (2001).

[16] V. V. Andreev and A. A. Pankov, Yad. Fiz. **75**, 67 (2012) [Phys. At. Nucl. **75**, 76 (2012)].

[17] V. M. Abazov *et al.* (D0 Collaboration), Phys. Lett. B **695**, 88 (2011).

[18] T. Aaltonen *et al.* (CDF Collaboration), Phys. Rev. Lett. **102**, 031801 (2009).

[19] G. Aad *et al.* (ATLAS Collaboration), Phys. Rev. D **85**, 032004 (2012).

[20] P. Langacker, Rev. Mod. Phys. **81**, 1199 (2009).

[21] T. G. Rizzo, arXiv:hep-ph/0610104.

[22] A. Leike, Phys. Rep. **317**, 143 (1999).

[23] K. Agashe, A. Azatov, T. Han, Y. Li, Z.-G. Si, and L. Zhu, Phys. Rev. D **81**, 096002 (2010).

[24] K. Agashe, H. Davoudiasl, S. Gopalakrishna, T. Han, G.-Y. Huang, G. Perez, Z.-G. Si, and A. Soni, Phys. Rev. D **76**, 115015 (2007).

[25] M. S. Carena, A. Daleo, B. A. Dobrescu, and T. M. P. Tait, Phys. Rev. D **70**, 093009 (2004).

[26] V. Barger, C.-W. Chiang, P. Langacker, and H.-S. Lee, Phys. Lett. B **580**, 186 (2004).

[27] D. Feldman, Z. Liu, and P. Nath, Phys. Rev. D **75**, 115001 (2007).
[28] A. Hebecker and J. March-Russell, Nucl. Phys. B **613**, 3 (2001).
[29] Y. Y. Komachenko and M. Y. Khlopov, Yad. Fiz. **51**, 1081 (1990) [Sov. J. Nucl. Phys. **51**, 692 (1990)].
[30] R. Martinez and F. Ochoa, Phys. Rev. D **80**, 075020 (2009).
[31] S. Chatrchyan *et al.* (CMS Collaboration), Phys. Rev. D **87**, 072002 (2013).
[32] G. Aad *et al.* (ATLAS Collaboration), J. High Energy Phys. 01 (2013) 116.
[33] ATLAS Collaboration, ATLAS-CONF-2012-129.
[34] J. Erler, P. Langacker, S. Munir, and E. Rojas, J. High Energy Phys. 08 (2009) 017.
[35] G. Aad *et al.* (ATLAS Collaboration), Phys. Rev. Lett. **107**, 272002 (2011).
[36] CMS Collaboration, Report No. CMS-PAS-EXO-12-015.
[37] R. Foot and X.-G. He, Phys. Lett. B **267**, 509 (1991).
[38] K. S. Babu, C. F. Kolda, and J. March-Russell, Phys. Rev. D **57**, 6788 (1998).
[39] C.-W. Chiang, Y.-F. Lin, and J. Tandean, J. High Energy Phys. 11 (2011) 083.
[40] J. L. Diaz-Cruz, J. M. Hernandez-Lopez, and J. A. Orduz-Ducuara, arXiv:1304.0016.
[41] J. Beringer *et al.* (Particle Data Group Collaboration), Phys. Rev. D **86**, 010001 (2012).
[42] T. Han, I. Lewis, R. Ruiz, and Z.-g. Si, Phys. Rev. D **87**, 035011 (2013).
[43] X. Gong, Z.-G. Si, S. Yang, and Y.-j. Zheng, Phys. Rev. D **87**, 035014 (2013).
[44] S.-S. Bao, X. Gong, H.-L. Li, S.-Y. Li, and Z.-G. Si, Phys. Rev. D **85**, 075005 (2012).
[45] S.-S. Bao, H.-L. Li, Z.-G. Si, and Y.-F. Zhou, Phys. Rev. D **83**, 115001 (2011).
[46] S. Gopalakrishna, T. Han, I. Lewis, Z.-g. Si, and Y.-F. Zhou, Phys. Rev. D **82**, 115020 (2010).
[47] G. Aad *et al.* (The ATLAS Collaboration), arXiv:0901.0512.
[48] G. L. Bayatian *et al.* (CMS Collaboration), J. Phys. G **34**, 995 (2007).